Biomimetic Fibers Made of Recombinant Spidroins with the Same Toughness as Natural Spider Silk

*Aniela Heidebrecht, Lukas Eisoldt, Johannes Diehl, Andreas Schmidt, Martha Geffers, Gregor Lang, and Thomas Scheibel**

Spider dragline silk exhibits extraordinary mechanical properties combining a moderate strength with good extensibility resulting in a toughness exceeding that of all other natural or synthetic fibers. Although spider silk has been in the focus of research since decades, the mechanical properties, especially the toughness, of reconstituted man-made fibers have never reached those of natural spider silk. The properties are based on the underlying spider silk proteins (spidroins), their self-assembly and their explicit processing. Here, two out of three pre-requisites for tough fibers are tackled; the contribution of individual spidroin domains to assembly is analyzed, and processing of recombinant spidroins into fibers is shown. Fiber toughness upon processing equals and even slightly exceeds that of natural ones dependent on both the underlying proteins and preparation (biomimetic self-assembly) of the silk dope, although the overall strength is lower based on the used and simplified single-protein set-up.

Spider dragline silk has for long been in the focus of materials' research mainly due to a toughness no other fiber can accomplish. Spider major ampullate (MA) silk fibers, aka dragline silk, show a core-shell-structure, with the core comprising proteinaceous fibrils covered by a three-layered shell of minor ampullate (MI) silk, glycoproteins and lipids, with only a minor role for the mechanical properties of the fibers.[1] The mechanics are mainly based on the protein fibrils comprising at least two proteins classified as MaSp1 and MaSp2 (MaSp, spidroin = spider fibroin), both of which are generally distinguished by their proline content, which is significantly higher in MaSp2.[2–4] MA spidroins have a molecular weight of 200–350 kDa[5,6] and are composed of a highly repetitive core domain flanked by amino- and carboxy-terminal domains with a distinct sequence. The core domain contains repeated (up to 100 times)[4,5] amino acid modules of 40–200 amino acids[3–5] composed of polyalanine stretches and glycine/proline-rich motifs. The strength of natural spider silk fibers is based on the polyalanine stretches stacked into β-sheets[7] resembling nanocrystallites which are embedded in an amorphous matrix,[1,8] based on the glycine/proline-rich areas and being responsible for the fiber's elasticity and flexibility.[9] The number of tandemly arrayed glycine/proline-rich motifs (GPGXX, X = predominantly tyrosine, leucine, glutamine)[4] is directly connected to the extensibility of silks. MaSp2 has nine consecutive GPGXX-motifs in a single repeat unit,[4] whereas flagelliform silk has at least 43 of these motifs in one unit[10] and is the most extensible spider silk with 200% of elongation.[2] Strikingly, the terminal domains are highly conserved between different spider species and even between silk types of individual spiders; they are composed of 100–150 amino acids and are folded into five-helix bundles.[11,12] The terminal domains are assembly triggers enabling the spidroin storage at high concentrations (up to 50% (w/v)) in the ampulla of the spinning gland (resembling the so-called spinning dope) and play an important role during initiation of fiber assembly.[13–16]

It has been hypothesized that pre-assembly of spidroins in the gland is the cause for lyotropic liquid crystal behavior in vivo.[17,18] Upon passage of the spinning dope through the tapered S-shaped spinning duct, sodium and chloride ions are replaced by potassium and more kosmotropic phosphate ions (inducing salting-out of the spidroins).[19,20] In combination with shear-stress, emerging from pulling the fibers from the spider's abdomen, the spidroins assemble into a nematic phase,[17] enabling formation and correct alignment of β-sheet-rich structures.[16] In vitro, during storage of the spidroins at pH 8.0 micellar-like structures can be detected, strictly depending on the presence of the carboxy-terminal domain[14] based on the fact that carboxy-terminal domains form disulfide-linked parallel dimers,[16] while the amino-terminal domains are monomeric at neutral pH.[21] Adding phosphate ions causes the nonrepetitive carboxy-terminal domain to partially refold and subsequently expose hydrophobic areas,[16] necessary to initiate fiber assembly. Further, upon decreasing the pH to ≈5.7, as found at the end of the spinning duct in vivo,[22] dimerization of the amino-terminal domain in an antiparallel manner is triggered in vitro,[22] yielding head-to-tail dimers enabling the formation of an endless network connecting the nanocrystalline β-sheet structures.[14–16,21]

Even though plenty of artificial spider silk fibers have been produced in the past using different recombinant or reconstituted spidroins and spinning-techniques, so far no fibers have been obtained with mechanical properties, i.e., toughness, even getting close to that of natural spider silk fibers.[23]

Here, we made use of previously established technologies to recombinantly produce spider silk-like proteins based on the sequence of garden spider (*A. diadematus*) MA spidroins. *A. diadematus* MA silk contains, in contrast to other investigated spider species, at least two MaSp2 proteins which are called *A. diadematus* fibroin 3 and 4 (ADF3 and ADF4). Here, based on

A. Heidebrecht, L. Eisoldt, J. Diehl, A. Schmidt, M. Geffers, G. Lang, Prof. T. Scheibel
Lehrstuhl Biomaterialien
Fakultät für Ingenieurwissenschaften
Universität Bayreuth
95440, Bayreuth, Germany
E-mail: thomas.scheibel@bm.uni-bayreuth.de

DOI: 10.1002/adma.201404234

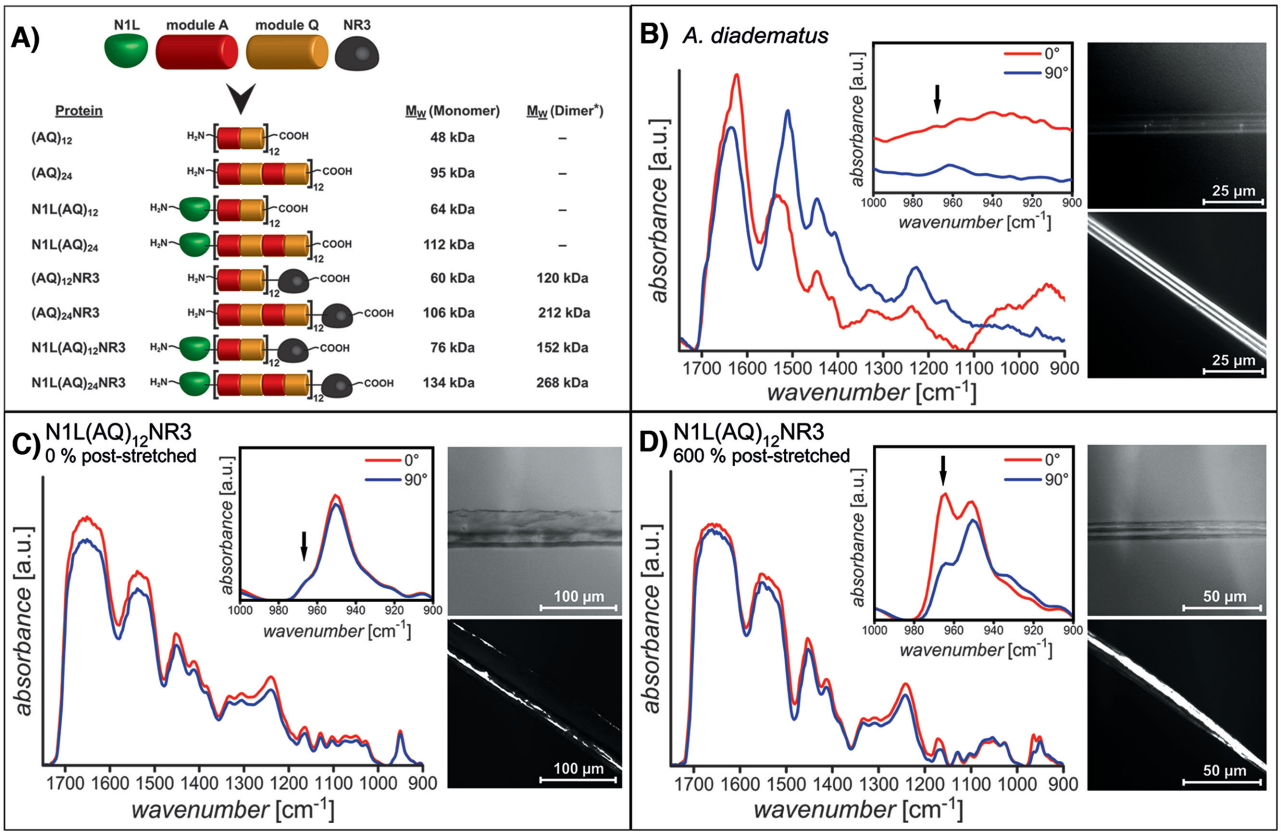

Figure 1. A) Scheme of the employed recombinant proteins, the sequences of the individual domains are derived from ADF3 (see the Supporting Information), one of the two identified MaSp2 components of *A. diadematus* dragline silk. The theoretical molecular weight (M_W, calculated using the ProtParam tool: http://web.expasy.org/protparam/) of the respective recombinant proteins is shown. *: Disulfide linked. B–D) Polarized FTIR spectra taken in parallel (0°, red) and perpendicular (90°, blue) to the fiber axis. (Inset) Enlargement of the absorption between 1000 and 900 cm^{-1}. The arrows in the insets mark the specific $(Ala)_n$ absorbance at ≈963 cm^{-1}; B) *A. diadematus* dragline silk, C) eADF3 ($N1L(AQ)_{12}NR3$)-fibers, 0% poststretched, D) eADF3 ($N1L(AQ)_{12}NR3$)-fibers, 600% poststretched.

consensus sequences of ADF3 (sequence accession number: AAC47010) eight engineered variants (eADF3) were designed for recombinant production in *E. coli*, varying in length/number of core repeats and presence/absence of the amino- and/or carboxy-terminal domains (**Figure 1**A), in order to investigate the impact of individual domains on storage, spinning dope conditions, assembly, and mechanical properties of fibers upon spinning.

Previously, the spinning dope has been identified as one highly important factor for spinning.[24] In nature, spider silk spinning dopes are highly concentrated (up to 50% (w/v)). Technically, such high concentrations can be achieved by stepwise concentrating solutions. "Classical" spinning dopes (CSD) were produced by simply removing excess water from the protein solution using dialysis against polyethylene glycol (PEG) yielding concentrations between 10% (w/v) to 17% (w/v). In order to prevent unspecific aggregation, 100×10^{-3} M NaCl was added to the buffered (50×10^{-3} M Tris/HCl, pH 8.0) solution prior to dialysis against PEG. Electrolytic conductivity measurements (Table S1, Supporting Information) showed no detectable amounts of salt after PEG-dialysis. Further, structural analysis of recombinant spider silk solutions before and after dialysis against PEG showed no change in protein structure.[25]

Dialysis of a solution with low protein concentration against a phosphate-containing buffer induced a liquid–liquid phase separation of eADF3 variants comprising the carboxy-terminal domain NR3 into a low density phase and a "self-concentrated" high density micellar phase[14] yielding a dope named "biomimetic" from now on. The addition of the phosphate ions induces a partial refolding of the carboxy-terminal domain, leading to initiation of protein assembly into micelles. Further, the presence of the carboxy-terminal domain is an important prerequisite for fiber self-assembly. Dynamic light scattering experiments on eADF3 high and low density phases revealed that the high density phase contains protein oligomers (M_W > 30 MDa), which were noncovalently associated, whereas the low density phase only showed dimeric proteins.[26]

While the phase-separated "biomimetic" spinning dopes (BSD) were stable for 3–5 days, the CSD gelled within a few hours due to nucleated fertilization of the proteins.[27,28]

Wet-spinning of CSD (before gelation started) by precipitation of the spidroins in a coagulation bath containing a mixture of water and isopropanol, as used previously,[29] typically yielded inhomogeneous fibers (Figure S1, Supporting Information) and sometimes short fiber fragments. The least homogeneous fibers were obtained from dopes comprising spidroins without

the carboxy-terminal domain ($(AQ)_{12}$, $(AQ)_{24}$, $N1L(AQ)_{12}$, $N1L(AQ)_{24}$). In contrast, spinning from BSD generally resulted in very homogeneous and long fibers. However, it was necessary to improve the performance of the fibers by poststretching. Du et al.[30] detected that the protein network structure (predominantly size and orientation of β-sheet crystals) changes substantially with the silk reeling speed and thus determines the mechanical properties of the silk fiber. In the natural spinning process the spider can control the reeling speed with its hind legs, poststretching the fiber as soon as it leaves the spinneret. While the formation of the liquid crystalline phase occurs quickly, the crystalline phase is formed slowly,[31] and this phase transition depends on the initial concentration and supersaturation of the silk protein solution. Upon shearing as well as poststretching, the protein chains are extended and thus getting closer to each other. As the local protein concentration is increased, crystal nucleation between the protein chains is triggered. A high reeling speed results in a high β-sheet crystal nucleus density, leading to fibers containing smaller crystallites, but with an increased crystal proportion.[30] Concerning the orientation of the β-sheet crystals, it was observed that a high reeling speed induces a better orientation of the β-sheet crystals along the thread axis.[30,32] Therefore, reeling and poststretching of the spider's silk fiber defines its mechanical properties. Similar observations were made with fibers from flexible polymers, where drawing and postdraw stretching led to better mechanical properties (e.g., higher tenacity) due to better strain alignment.[33] In our set-up, the recombinant fibers were stretched up to 600% of their initial length directly after spinning to align the spidroins. The diameter of poststretched fibers spun from BSD was uniform throughout each individual fiber with a mean diameter variation <5%. Approximately 5% of fibers spun from BSD were disposed due to defects or inhomogeneity, while poststretched fibers which were spun from CSD contained approximately 15% inhomogeneous or defective fibers. Polarized Fourier transformation infrared (FTIR) spectroscopy was used in parallel (0°) and perpendicular (90°) to the fiber axis to determine the alignment of the β-sheet stacks in the fibers (Figure 1, B–D). The absorption peak at ≈963 cm^{-1} corresponds to a highly specific coupled main- and side chain stretching (CH_3 rock, N–Cα stretch)[20] of the β-sheet forming $(Ala)_n$ sequences.

The intensity of the $(Ala)_n$ peak at 963 cm^{-1} in *A. diadematus* dragline fibers is significantly higher in parallel than perpendicular to the fiber axis, demonstrating the alignment of the $(Ala)_n$ β-sheet stacks along the fiber axis. The polarized FTIR spectra of the recombinant spider silk fibers showed a similar result, but only in poststretched ones, confirming the impact of shear stress on structure alignment. Tensile testing of all recombinant spidroin fibers showed that poststretching also significantly improved the mechanical properties, while as-spun fibers without structural alignment (0% poststretching) appeared to be very brittle (**Figure 2**).

The differences in mechanics upon stretching depended on a) the molecular set-up of the recombinant spidroins and, even more importantly, b) the dope preparation. $(AQ)_{12}$-fibers spun from CSD were very brittle and poststretching was only possible up to 400% of the initial length without breaking

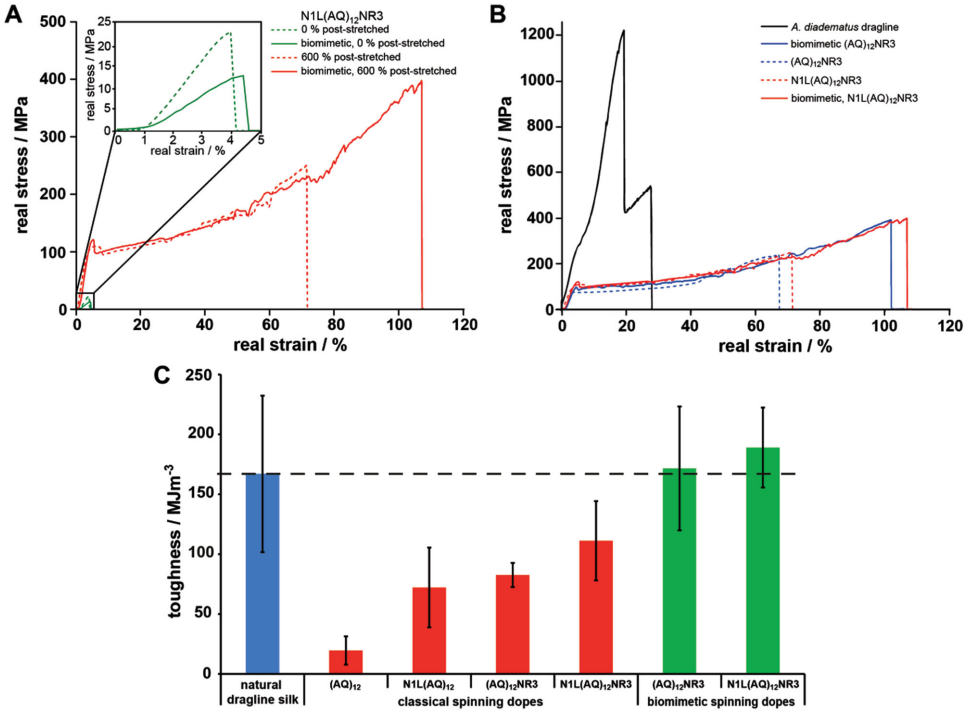

Figure 2. A,B) Real stress–real strain curves of recombinant and natural spider silk fibers. A) As-spun (inset) and 600% poststretched $N1L(AQ)_{12}NR3$-fibers, spun from "classical" (CSD) as well as "biomimetic" (BSD) spinning dopes (both 10% (w/v)) and B) 600% poststretched $(AQ)_{12}NR3$- and $N1L(AQ)_{12}NR3$-fibers from CSD as well as BSD in comparison to natural *A. diadematus* dragline silk fibers. C) Average toughness of natural dragline silk fibers (blue), fibers spun from CSD (red) and BSD (green).

Table 1. Mechanical properties of natural and recombinant spider silk fibers. (A, B) CSD (all variants) and (C) BSD (variants with carboxy-terminal domain only). Tensile testing was performed at 30% rH.

A								
Protein	$(AQ)_{12}$		$(AQ)_{24}$		$N1L(AQ)_{12}$		$N1L(AQ)_{24}$	
Stretching [%]	0	400	0	600	0	400	0	300
Diameter [μm]	35 ± 7	15 ± 5	70 ± 7	22 ± 2	42 ± 6	15 ± 2	78 ± 21	55 ± 9
Extensibility [%]	17 ± 9	38 ± 16	22 ± 3	65 ± 6	8 ± 1	51 ± 17	6 ± 2	10 ± 6
Strength [MPa]	10 ± 2	66 ± 22	22 ± 4	280 ± 48	19 ± 3	212 ± 53	15 ± 3	24 ± 7
Toughness [MJ m^{-3}]	0.9 ± 0.4	20 ± 12	4 ± 1	110 ± 24	1 ± 0.4	72 ± 33	0.4 ± 0.2	2 ± 1
Young's modulus [GPa]	0.9 ± 0.4	2 ± 0.9	0.4 ± 0.1	4 ± 0.6	0.5 ± 0.1	4 ± 0.9	0.7 ± 0.2	1 ± 0.3

B								
Protein	$(AQ)_{12}NR3$		$(AQ)_{24}NR3$		$N1L(AQ)_{12}NR3$		$N1L(AQ)_{24}NR3$	
Stretching [%]	0	600	0	600	0	600	0	600
Diameter [μm]	59 ± 8	23 ± 3	57 ± 0	30 ± 5	57 ± 3	24 ± 7	62 ± 8	27 ± 4
Extensibility [%]	10 ± 3	64 ± 11	5 ± 1	50 ± 12	4 ± 2	82 ± 13	8 ± 2	47 ± 14
Strength [MPa]	32 ± 12	244 ± 23	29 ± 2	161 ± 65	21 ± 8	251 ± 57	22 ± 3	180 ± 50
Toughness [MJ m^{-3}]	2 ± 1.5	83 ± 10	0.6 ± 0.1	49 ± 26	0.4 ± 0.1	111 ± 33	0.8 ± 0.4	50 ± 13
Young's modulus [GPa]	2 ± 0.5	4 ± 0.4	1 ± 0.2	3 ± 0.7	0.9 ± 0.4	3 ± 0.5	0.8 ± 0.2	4 ± 0.5

C									
Protein	$(AQ)_{12}NR3$		$(AQ)_{24}NR3$		$N1L(AQ)_{12}NR3$		$N1L(AQ)_{24}NR3$		Natural dragline silk
Stretching [%]	0	600	0	600	0	600	0	600	N/A[a]
Diameter [μm]	39 ± 6	26 ± 6	56 ± 1	21 ± 5	155 ± 8	27 ± 10	75 ± 14	20 ± 6	4 ± 0.4[b]
Extensibility [%]	7 ± 2	95 ± 24	7 ± 3	44 ± 13	6 ± 1	110 ± 25	7 ± 2	54 ± 15	24 ± 8[b]
Strength [MPa]	54 ± 16	383 ± 113	23 ± 4	355 ± 92	13 ± 2	370 ± 59	25 ± 5	308 ± 131	1183 ± 334[b]
Toughness [MJ m^{-3}]	2 ± 0.8	172 ± 52	0.7 ± 0.6	83 ± 18	0.3 ± 0.1	189 ± 33	0.8 ± 0.4	90 ± 29	167 ± 65
Young's modulus [GPa]	2 ± 0.9	3 ± 2	0.8 ± 0.3	5 ± 2	0.5 ± 0.1	4 ± 1	0.9 ± 0.2	5 ± 2	8 ± 2

[a]Not applicable; [b]Values correspond to rupture of a single filament (not to the naturally occurring brin).

of the fibers. In contrast, $N1L(AQ)_{12}$- and $(AQ)_{12}NR3$-fibers spun from CSD showed a higher extensibility and strength resulting in a higher toughness than the corresponding $(AQ)_{12}$-fibers (**Table 1**). Like with $(AQ)_{12}$-fibers, poststretching of $N1L(AQ)_{12}$-fibers spun from CSD was only possible up to 400% of the initial length, whereas $(AQ)_{12}NR3$-fibers spun from CSD could be poststretched up to 600% (Table 1A). The strength and toughness of the poststretched $N1L(AQ)_{12}$-fibers increased more than 3-fold, and that of $(AQ)_{12}NR3$-fibers increased 4-fold in comparison to the poststretched $(AQ)_{12}$-fibers (Figure 2C). In that set of experiments, the highest toughness (111 MJ m^{-3}) was obtained with poststretched $N1L(AQ)_{12}NR3$-fibers. While showing the same strength, $N1L(AQ)_{12}NR3$-fibers were significantly more extensible ($p = 0.0030$) and less stiff (lower young's modulus ($p = 0.0009$)) than $(AQ)_{12}NR3$-fibers.

Next, fibers were spun using self-assembled, phase-separated (biomimetic) spinning dopes (BSD). In this set-up, self-assembly determined the final concentration of the spinning dopes in a regime between 10%–15% (w/v). Poststretched "biomimetic" $(AQ)_{12}NR3$-, and $N1L(AQ)_{12}NR3$-fibers showed a significant increase in extensibility and toughness in comparison to the poststretched fibers spun from CSD (Figure 2C), yielding a toughness equal ($(AQ)_{12}NR3$, 171.6 ± 51.7 MJ m^{-3}) or even slightly superior ($N1L(AQ)_{12}NR3$, 189.0 ± 33.4 MJ m^{-3}) to natural spider silk fibers (167.0 ± 65.3 MJ m^{-3}).

Since typically the molecular weight influences the mechanical properties of polymer fibers,[34] fibers were also spun using $(AQ)_{24}$-derivatives with a doubled molecular weight in comparison to $(AQ)_{12}$-derivatives. As expected for a "plain" polymer, $(AQ)_{24}$-fibers spun from CSD showed improved mechanical properties in comparison to $(AQ)_{12}$-fibers, such as a 1.5-fold increase in extensibility and a 4-fold increase in strength, resulting in a 5-fold increase in toughness. However, in presence of the folded amino- or carboxy-terminal domains N1L/NR3 the effects were no longer dominated by molecular weight of the underlying proteins but obviously by their assembly features. All fibers spun from $N1L(AQ)_{24}$, $(AQ)_{24}NR3$, and $N1L(AQ)_{24}NR3$ (CSD) revealed substantially inferior mechanical properties to the corresponding $(AQ)_{24}$-fibers (Table 1A,B), indicating a substantial "protein"-influence on the silk polymer. $N1L(AQ)_{24}$-fibers were very brittle, and poststretching was only possible up to 300% of the initial length. As the aminoterminal domain of the spidroins only dimerizes upon a pH change during the spinning process, it is still in its monomeric form in the spinning dope, thus preventing a correct alignment of the repetitive part of the protein molecules, especially in the absence of the dimerized carboxy-terminal domain, resulting

Table 2. Roles of spidroins terminal domains.

	Non-repetitive amino-terminal domain	Non-repetitive carboxy-terminal domain
Spinning dope	High impact: monomeric during storage, folded domain inhibits protein aggregation; crucial in order to obtain an intermolecular protein network	High impact: dimerized/assembled domain renders protein less prone to unspecific aggregation; crucial for protein assembly into micellar structures and self-assembly to BSD
Assembly	High impact: dimerization occurs upon acidification, step-wise initiation of fiber assembly	High impact: initiation of fiber assembly
Mechanical properties of fibers	No direct impact: indirect influence due to impact on assembly and spinning dope	No direct impact: only indirect influence due to high impact on assembly

in brittle fibers (**Table 2**). In comparison to N1L$(AQ)_{24}$ fibers, $(AQ)_{24}$NR3 and N1L$(AQ)_{24}$NR3 fibers had a 5-fold increased extensibility and strength and a 30-fold increased toughness (Table 1A,B).

Again, similar to the findings with $(AQ)_{12}$-derivatives, the mechanical properties of $(AQ)_{24}$NR3-fibers spun from BSD showed a significant increase in strength and toughness compared to $(AQ)_{24}$NR3-fibers spun from CSD. Likewise, N1L$(AQ)_{24}$NR3-fibers spun from BSD showed a significantly higher strength (307.5 MPa) and toughness (89.6 MJ m^{-3}) than fibers spun from the corresponding CSD (180.0 MPa, 50.3 MJ m^{-3}). Unexpectedly, the overall mechanical properties of the $(AQ)_{24}$-derivatives containing either one or both terminal domains were much lower than that of the $(AQ)_{12}$-derivatives from both CSD and BSD, likely due to incorrect higher order assembly of the individual chains in the spinning dope. It is likely that once the assembly-controlling terminal domains are present, the large repetitive unit of the $(AQ)_{24}$-derivatives causes entanglement of the molecules. Additionally, intermolecular interactions of the nonrepetitive terminal domains in the micellar structures prevent a perfect alignment as it is known for classical polymers. These entanglements cannot be straightened out during the used limited and nonbiomimetic wet-spinning process. In the natural spinning process, the preassembled proteins are gradually exposed to the pH drop as well as the shear forces, supporting their correct assembly into fibers. Clearly, to overcome the entanglement of the repetitive unit, a biomimetic spinning process will have to be developed for future experiments, tackling the third of three prerequisites: i) underlying spidroins, ii) their self-assembly, and iii) their explicit processing for natural spider silk formation.

The obtained results underline that the domain-set-up as well as prestructuring/preassembly of spidroins in the spinning dope (both resembling a "protein feature") have a highly significant impact on the mechanical properties of the spun fibers. During wet-spinning their impact even supersedes that of the molecular weight of the protein (resembling a "polymer feature"). Phosphate-induced self-assembly/pre-structuring of recombinant spidroins in spinning dopes initiates the formation of an extended intermolecular protein network necessary for the extraordinary mechanical properties of the fibers. Strikingly, the toughness of recombinant silk fibers spun from $(AQ)_{12}$NR3 and N1L$(AQ)_{12}$NR3 BSD equals that of the so far unmatched natural spider silk fibers. The highest mean toughness (189 MJ m^{-3}) was obtained with poststretched fibers wet-spun from biomimetic N1L$(AQ)_{12}$NR3 spinning dopes, even slightly exceeding the toughness (on average) of natural spider silk fibers. This toughness is based on the fact that the engineered fibers are not as strong as natural fibers, but far more extensible, which relies on the properties of the employed proline-rich MaSp2-analogue. Important differences between the used set-up and the natural blueprint are: i) the simple one-protein system (in nature the fibers are composed of at least two different major ampullate spidroins with different sequences and protein features), and ii) the simple wet-spinning process (in comparison to the complex natural spinning process). Combination of more than one recombinant spidroin, as well as the development of a biomimetic spinning technology will likely allow to achieve fibers with mechanical properties superior to that of spiders in the future, opening routes to so far none achievable fibrous materials.

Experimental Section

Protein Production: The genes encoding recombinant spider silk proteins eADF3 $(AQ)_{12}$, $(AQ)_{24}$, $(AQ)_{12}$NR3, $(AQ)_{24}$NR3, N1L$(AQ)_{12}$, and N1L$(AQ)_{24}$ were cloned, expressed, and the proteins were purified as previously described.[12] N1L$(AQ)_{12}$NR3 and N1L$(AQ)_{24}$NR3 were produced using the SUMO system[35] and purified using nickel affinity chromatography, followed by cleavage of the SUMO-TAG and ammonium sulfate precipitation.

Spinning Dope Preparation: The lyophilized proteins were dissolved in 6 M GdmSCN and dialyzed against 50×10^{-3} M Tris/HCl, pH 8.0, 100×10^{-3} M NaCl, using dialysis membranes with a molecular weight cut-off of 6000–8000 Da. CSD were prepared by dialysis against a 20% (w/v) PEG (35 kDa) solution, and BSD were prepared by dialysis against 30×10^{-3}–50×10^{-3} M sodium phosphate buffer, pH 7.2.

Fiber Production: Spinning dopes were extruded through a syringe into a large beaker filled with a coagulation bath. After fiber formation the fibers were taken out of the bath and manually poststretched in an additional bath. For wet-spinning and poststretching (if applicable) coagulation baths were used containing a mixture of water and isopropanol, as described previously.[29] *A. diadematus* (body weight: 300–600 mg) were fed with blowflies, and fibers were obtained by forcibly silking an adult *A. diadematus* at 160 mm s^{-1}.

Fiber Analysis: The fibers were analyzed with an optical microscope (Leica DMI3000B), and fibers showing defects were disposed. Fiber diameters were determined using 20×, 40×, and 100× object lenses and the software Leica V4.3. Birefringence was detected using polarizers at 0°, 45°, and 90° and pictures were obtained with the camera Leica DMC2900. For scanning electron microscopy (SEM, Zeiss LEO 1530, 3 kV), fiber samples and fiber breaking edges were sputtered with a 2 nm platinum coating (Cressington 208HR high-resolution sputter coater) before imaging. Fourier transformation infrared (FTIR) spectroscopy measurements of the fibers were performed using a Bruker Tensor 27 (Bruker Optics, Ettlingen, Germany) with a Hyperion 1000 FTIR microscope. Alignment of the β-sheet crystals was analyzed using a 15× object lens with polarizing filters at 0° and 90° in transmission mode (IR polarizers supplied by Optometrics Corporation). Spectra were plotted using Origin 8.1G (OriginLab Corporation, Northampton, MA, USA).

Tensile Testing: For tensile testing fiber pieces were mounted onto plastic sample holders with a 2 mm gap using superglue (UHU GmbH & Co. KG). Tensile testing was performed using a BOSE Electroforce 3220 with a 0.49 N load cell and a pulling rate of 0.04 mm s^{-1} at 30%

relative humidity. Mechanical data were calculated considering real stress and real strain data and using Microsoft Excel 2010 (Microsoft Corporation, Redmond, WA, USA). For statistical analysis an unpaired two-sided *t*-test was performed for groups with similar variances and sample numbers were ≥10, except for poststretched N1L(AQ)$_{12}$NR3 fibers spun from CSD ($n = 7$).

Supporting Information

Supporting Information is available from the Wiley Online Library or from the author.

Acknowledgements

The authors thank Martina Elsner and Hendrik Bargel for SEM images. A.H. kindly appreciates financial support by the "Universität Bayern, e.V., Graduiertenförderung nach dem bayerischen Eliteförderungsgesetz". This work was financially supported by DFG grant SFB 840 TP A8 (to T.S.), DFG SCHE 603/4 and the Technologieallianz Oberfranken (TAO).

Received: September 12, 2014
Revised: January 13, 2015
Published online: February 16, 2015

[1] A. Sponner, W. Vater, S. Monajembashi, E. Unger, F. Grosse, K. Weisshart, *PLoS One* **2007**, *2*, e998.
[2] C. Y. Hayashi, N. H. Shipley, R. V. Lewis, *Int. J. Biol. Macromol.* **1999**, *24*, 271.
[3] a) P. A. Guerette, D. G. Ginzinger, B. H. Weber, J. M. Gosline, *Science* **1996**, *272*, 112; b) K. W. Sanggaard, J. S. Bechsgaard, X. Fang, J. Duan, T. F. Dyrlund, V. Gupta, X. Jiang, L. Cheng, D. Fan, Y. Feng, L. Han, Z. Huang, Z. Wu, L. Liao, V. Settepani, I. B. Thøgersen, B. Vanthournout, T. Wang, Y. Zhu, P. Funch, J. J. Enghild, L. Schauser, S. U. Andersen, P. Villesen, M. H. Schierup, T. Bilde, J. Wang, *Nat. Commun.* **2014**, *5*, 1.
[4] M. B. Hinman, R. V. Lewis, *J. Biol. Chem.* **1992**, *267*, 19320.
[5] N. A. Ayoub, J. E. Garb, R. M. Tinghitella, M. A. Collin, C. Y. Hayashi, *PLoS One* **2007**, *2*, e514.
[6] a) G. C. Candelas, J. Cintron, *J. Exp. Zool.* **1981**, *216*, 1; b) C. Jackson, J. P. O'Brien, *Macromolecules* **1995**, *28*, 5975.
[7] B. L. Thiel, C. Viney, *Science* **1996**, *273*, 1480.
[8] a) J. Perez-Rigueiro, M. Elices, G. R. Plaza, G. V. Guinea, *Macromolecules* **2007**, *40*, 5360; b) A. Sponner, E. Unger, F. Grosse, K. Weisshart, *Nat. Mater.* **2005**, *4*, 772.
[9] a) A. E. Brooks, H. B. Steinkraus, S. R. Nelson, R. V. Lewis, *Biomacromolecules* **2005**, *6*, 3095; b) Y. Liu, A. Sponner, D. Porter, F. Vollrath, *Biomacromolecules* **2008**, *9*, 116; c) K. Ohgo, T. Kawase, J. Ashida, T. Asakura, *Biomacromolecules* **2006**, *7*, 1210.
[10] C. Y. Hayashi, R. V. Lewis, *J. Mol. Biol.* **1998**, *275*, 773.
[11] a) R. J. Challis, S. L. Goodacre, G. M. Hewitt, *Insect Mol. Biol.* **2006**, *15*, 45; b) M. Hedhammar, A. Rising, S. Grip, A. S. Martinez, K. Nordling, C. Casals, M. Stark, J. Johansson, *Biochemistry* **2008**, *47*, 3407; c) A. Rising, G. Hjalm, W. Engstrom, J. Johansson, *Biomacromolecules* **2006**, *7*, 3120.
[12] D. Huemmerich, C. W. Helsen, S. Quedzuweit, J. Oschmann, R. Rudolph, T. Scheibel, *Biochemistry* **2004**, *43*, 13604.
[13] a) G. Askarieh, M. Hedhammar, K. Nordling, A. Saenz, C. Casals, A. Rising, J. Johansson, S. D. Knight, *Nature* **2010**, *465*, 236; b) L. Eisoldt, A. Smith, T. Scheibel, *Mater. Today* **2011**, *14*, 80.
[14] L. Eisoldt, J. G. Hardy, M. Heim, T. R. Scheibel, *J. Struct. Biol.* **2010**, *170*, 413.
[15] L. Eisoldt, C. Thamm, T. Scheibel, *Biopolymers* **2012**, *97*, 355.
[16] F. Hagn, L. Eisoldt, J. G. Hardy, C. Vendrely, M. Coles, T. Scheibel, H. Kessler, *Nature* **2010**, *465*, 239.
[17] a) D. P. Knight, F. Vollrath, *Philos. Trans. R. Soc. London, Ser. B* **2002**, *357*, 219; b) F. N. Braun, C. Viney, *Int. J. Biol. Macromol.* **2003**, *32*, 59.
[18] L. Onsager, *Ann. Ny. Acad. Sci.* **1949**, *51*, 627.
[19] D. P. Knight, F. Vollrath, *Naturwissenschaften* **2001**, *88*, 179.
[20] P. Papadopoulos, J. Sölter, F. Kremer, *Eur. Phys. J. E: Soft Matter Biol. Phys.* **2007**, *24*, 193.
[21] a) F. Hagn, C. Thamm, T. Scheibel, H. Kessler, *Angew. Chem. Int. Ed.* **2011**, *50*, 310; b) F. Hagn, C. Thamm, T. Scheibel, H. Kessler, *Angew. Chem.* **2011**, *123*, 324.
[22] N. Kronqvist, M. Otikovs, V. Chmyrov, G. Chen, M. Andersson, K. Nordling, M. Landreh, M. Sarr, H. Jornvall, S. Wennmalm, J. Widengren, Q. Meng, A. Rising, D. Otzen, S. D. Knight, K. Jaudzems, J. Johansson, *Nat. Commun.* **2014**, *5*, 3254.
[23] A. Heidebrecht, T. Scheibel, *Adv. Appl. Microbiol.* **2013**, *82*, 115.
[24] S. Arcidiacono, C. M. Mello, M. Butler, E. Welsh, J. W. Soares, A. Allen, D. Ziegler, T. Laue, S. Chase, *Macromolecules* **2002**, *35*, 1262.
[25] a) M. Humenik, T. Scheibel, *ACS Nano* **2014**, *8*, 1342; b) K. Schacht, T. Jüngst, M. Schweinlin, A. Ewald, J. Groll, T. Scheibel, *Angew. Chem. Int. Ed.* **2015**, *54*, DOI: 10.1002/ange.201409846.
[26] a) J. H. Exler, D. Hummerich, T. Scheibel, *Angew. Chem. Int. Ed.* **2007**, *46*, 3559; b) J. H. Exler, D. Hummerich, T. Scheibel, *Angew. Chem.* **2007**, *119*, 3629.
[27] K. Schacht, T. Scheibel, *Biomacromolecules* **2011**, *12*, 2488.
[28] M. Humenik, M. Magdeburg, T. Scheibel, *J. Struct. Biol.* **2014**, *186*, 431.
[29] F. Teule, W. A. Furin, A. R. Cooper, J. R. Duncan, R. V. Lewis, *J. Mater. Sci.* **2007**, *42*, 8974.
[30] N. Du, X. Y. Liu, J. Narayanan, L. Li, M. L. M. Lim, D. Li, *Biophys. J.* **2006**, *91*, 4528.
[31] C. Viney, A. E. Huber, D. L. Dunaway, K. Kerkam, S. T. Case, in *Silk Polymers. Materials Science and Biotechnology*, (Eds: D. L. Kaplan, W. W. Adams, B. Farmer, C. Viney) American Chemical Society, Washington D.C. **1994**, pp. 120–136.
[32] C. Riekel, B. Madsen, D. Knight, F. Vollrath, *Biomacromolecules* **2000**, *1*, 622.
[33] T. Ohta, *Polym. Eng. Sci.* **1983**, *23*, 697.
[34] a) T. A. Hancock, J. E. Spruiell, J. L. White, *J. Appl. Polym. Sci.* **1977**, *21*, 1227; b) P. Gupta, C. Elkins, T. E. Long, G. L. Wilkes, *Polymer* **2005**, *46*, 4799.
[35] a) T. R. Butt, S. C. Edavettal, J. P. Hall, M. R. Mattern, *Protein Expression Purif.* **2005**, *43*, 1; b) J. G. Marblestone, S. C. Edavettal, Y. Lim, P. Lim, X. Zuo, T. R. Butt, *Protein Sci.* **2006**, *15*, 182.